Engineering Structures 244 (2021) 112766

Contents lists available at ScienceDirect

Engineering Structures

journal homepage: www.elsevier.com/locate/engstruct

Seismic design coefficients and factors for coupled composite plate shear walls/concrete filled (CC-PSW/CF)

Emre Kizilarslan [a,*], Morgan Broberg [b], Soheil Shafaei [b], Amit H. Varma [b], Michel Bruneau [a]

[a] Dept. of Civil Structural and Environmental Engineering, University at Buffalo, Buffalo, NY 14260, United States
[b] Lyles School of Civil Engineering, Purdue University, West Lafayette, IN 47907, United States

ARTICLE INFO

Keywords:
Coupled composite plate shear walls
Composite plate shear walls
Coupling beams
Seismic performance
Collapse
Collapse fragility curves
Seismic performance factors
FEMA P695 methodology
Seismic effects

ABSTRACT

ASCE 7–16 (2016) [4] defines three seismic performance factors to approximately predict the inelastic response of a seismic resisting system. These factors are the response modification factor, R; deflection amplification factor, C_d; and the system over-strength factor, Ω_o. The research presented here was conducted, using FEMA P695 methodology, to determine the value of the above factors for a special seismic-force resisting system defined as Coupled Composite Plate Shear Walls-Concrete Filled (CC-PSW/CF). The ASCE 7–16 (2016) [4] and AISC 341–16 (2016) seismic provisions provide specific requirements for the use of planar composite steel plate shear walls in seismic regions. However, the ASCE-7–16 standard does not differentiate between coupled and non-coupled walls. Coupled walls can benefit from the added energy dissipation provided by their coupling beams and are accordingly expected to exhibit better seismic hysteretic behavior than uncoupled walls. Therefore, coupled walls systems should arguably have a higher response modification factor value. In this paper, the FEMA P695 approach taken for determining the seismic parameters of CC-PSW/CF is presented. To enhance confidence in the results, the Incremental Dynamic Analyses needed as part of the P695 procedure were conducted in parallel using two different non-linear hysteretic models. Complementary studies were also conducted to investigate the sensitivity of results to assumptions related to damping and yielding models. Results show that values $R = 8$, $C_d = 5.5$, and $\Omega_o = 2.5$ would be appropriate for CC-PSW/CF.

1. Introduction

ASCE 7-16 [4] defines three seismic performance factors to approximately predict the inelastic response of a seismic resisting system. These factors are the response modification factor, R; deflection amplification factor, C_d; and the system over-strength factor, Ω_o. The design response spectrum specified by ASCE 7–16 [4] is based on the dynamic response of an elastic SDOF system with 5% damping. Therefore, the base shear calculated from the spectrum is divided by the R-factor to obtain design seismic force of a ductile structure allowed to undergo inelastic response. The second factor, C_d, serves to multiply the deflections obtained from the elastic analysis performed using the reduced base shear in order to estimate the actual ultimate inelastic deflection of the structure. Also, to account for factors that increase lateral load resistance beyond the point of first yield point as lateral load increases, the reduced base shear is multiplied by another factor, namely the over-strength factor (Ω_o), to approximate the strength corresponding to development of the full plastic mechanism of the entire structural system. ASCE 7–16 [4] specifies values for these factors for different seismic force-resisting systems.

One of the structural systems for which ASCE 7–16 provides the above seismic performance factors is Composite Plate Shear Walls – Concrete Filled (C-PSW/CF). C-PSW/CF are walls that consist of two steel plates with concrete infilled between them. The steel plates are connected to each other using tie bars that are embedded in the concrete infill and, in some instances, steel-headed stud anchors. The steel plates serve as the primary reinforcement for the concrete infill and provide stay-in-place formwork during construction. The concrete infill also prevents inward local buckling of the steel plates thus improving their stability [2,15].

ASCE 7–16 [4] refers to the AISC 341–16 (2016) seismic provisions for specific requirements for the use of planar composite steel plate shear walls in seismic regions. However, ASCE-7–16 does not differentiate between coupled and non-coupled walls. Coupled Composite Plate Shear

* Corresponding author.
E-mail addresses: emrekizi@buffalo.edu (E. Kizilarslan), mbroberg@purdue.edu (M. Broberg), sshafaei@purdue.edu (S. Shafaei), ahvarma@purdue.edu (A.H. Varma), bruneau@buffalo.edu (M. Bruneau).

https://doi.org/10.1016/j.engstruct.2021.112766
Received 6 November 2020; Received in revised form 7 May 2021; Accepted 22 June 2021
Available online 23 July 2021

Table 1
Archetype performance group summary table.

Performance Group Summary				
Group No.	Grouping Criterial			Number of Archetypes
	Basic Configuration	Design Load Level		
		Gravity	Seismic Design Category (SDC)	
PG-1	Type I	Typical	D_{max}	6 (8 & 12 Story)
PG-2			D_{min}	2 (8 & 12 Story)
PG-3	Type II	Typical	D_{max}	6 (18 & 22 story)
PG-4			D_{min}	2 (18 & 22 story)

Walls-Concrete Filled (CC-PSW/CF) consists of two C-PSW/CFs linked together by coupling beams at floor levels. The coupling beams are also filled composite tubes. Coupled walls can benefit from the added energy dissipation provided by their coupling beams and are accordingly expected to exhibit better seismic hysteretic behavior than uncoupled walls. Arguably, CC-PSW/CF should have better seismic performance factors than C-PSW/CF.

The aim of the research presented here was to determine the appropriate R-factor (and other corresponding seismic response parameters, C_d and Ω_o) for CC-PSW/CF. The FEMA P695 procedure (2009)

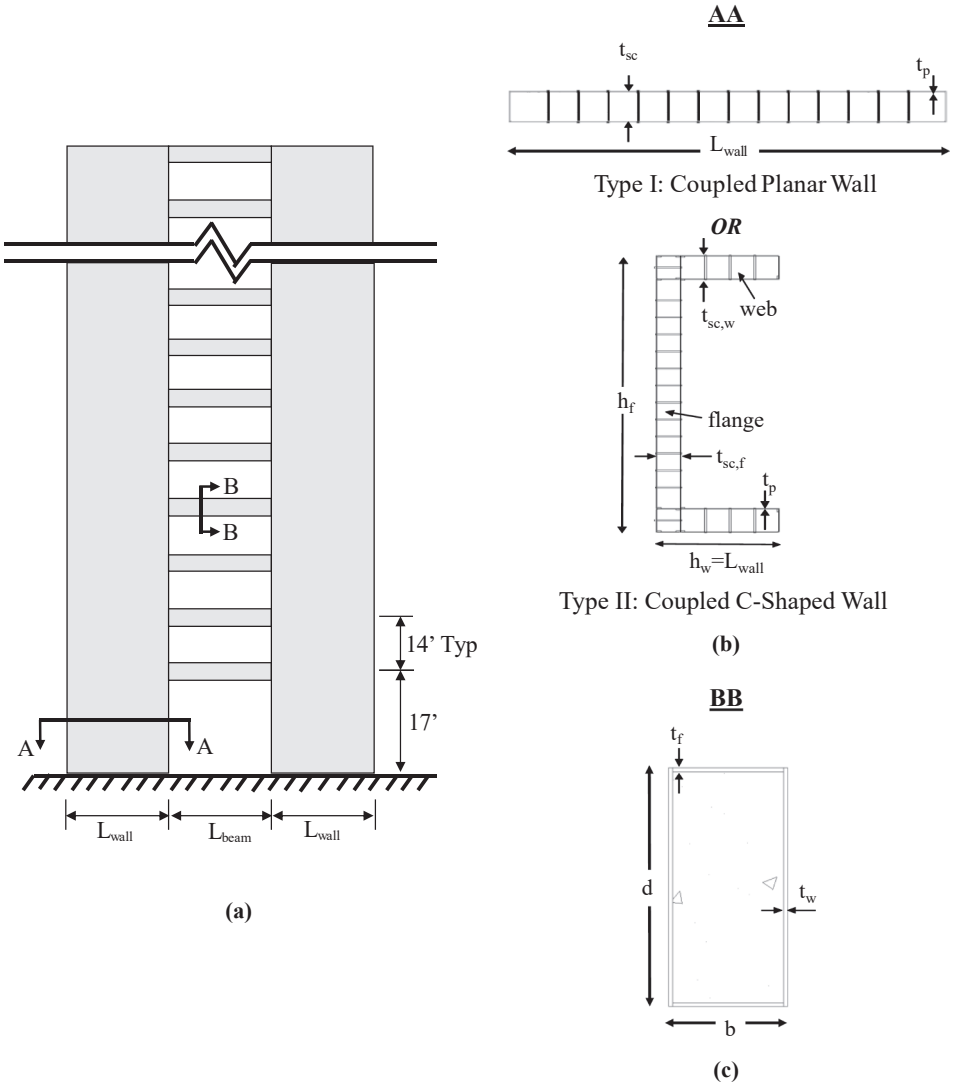

Fig. 1. Designed CC-PSW/CF archetypes in (a) elevation view, (b) plan views of planar walls (Type I) or C-Shaped walls (Type II), and; (c) cross-section of coupling beams.

was used for this purpose. The FEMA P695 procedure is intended to ensure that an adequate margin against collapse exists for the maximum considered earthquake (MCE) hazard, as established by performing a large number of nonlinear earthquake analysis (i.e., incremental dynamic analysis) for a significant set of strong earthquake records. Given that coupled C-PSW/CF is a relatively new structural system, it was also decided in this study to perform the incremental dynamic analyses required by the FEMA P695 procedure using two different set of nonlinear hysteretic models, as a way to gage the sensitivity of response to changes in numerical models and enhance confidence in the final results (e.g., one model used distributed plasticity fiber hinges, while the other used concentrated plastic hinges, both calibrated against experimental results). The findings of this study are intended to substantiate proposed revised R-values in subsequent editions of ASCE 7.

2. FEMA P695 methodology

The FEMA P695 procedure (2009) relies on inelastic nonlinear time history analysis to determine response of structural system archetypes using Incremental Dynamic Analysis (IDA) for a suite of ground motions, comparison of their response with demand for Maximum Considered Earthquake (MCE), and probabilistic evaluation of their collapse risk. The methodology provides a rational basis to quantify seismic performance factors, namely: response modification coefficient (R factor), system over-strength factor (Ω_o factor), and deflection amplification factor (C_d factor). Key steps of the methodology for establishing these factors include: 1) development of archetype buildings having the structural system under consideration; 2) development of nonlinear analytical models that appropriately captures the hysteretic behavior of the structural elements considered, including strength and stiffness degradation; 3) nonlinear static and dynamic analyses (i.e., pushover and incremental dynamic analyses), and; 4) performance evaluation of the system under consideration in terms of probabilistic collapse assessment under MCE ground motions.

The most important step in the FEMA P695 methodology (2009) is the development of accurate structural models to simulate the component strength and stiffness deterioration. As mentioned above, two different modelling approach were taken here (these differences will be described in details in a subsequent section). As the details of specific non-linear models that can be used to calculate the hysteretic response of CC-PSW/CF involve a number of complexities, and requires calibration and validation against experimental results, a thorough description of these models and their calibration/validation has been provided in a prior publication [8,11]. Building on the results reported in the companion paper, focus here is on the steps and results of the seismic performance assessments, including the development of CC-PSW/CF archetypes, the results of nonlinear static and dynamic analyses (i.e., pushover and incremental dynamic analyses), and the evaluation of collapse performance. Moreover, also presented are results from additional complementary analyses conducted to investigate the sensitivity of the results to different assumptions on damping ratios and plastic hinge length.

3. Development of archetypes

The design of the archetypes focuses on low to mid-rise office buildings (8–22 stories). Based on FEMA P695 recommendations, only the lateral load resisting system (core wall) is designed in this task. A set of initial parameters and a design procedure was developed prior to designing these structures. The initial parameters were developed in consultation with a project review panel (identified in the acknowledgments) as the research team desired to design archetype structures using a similar approach to industry professionals and previous FEMA P695 studies. For example, the coupled walls were assumed to be occupy one full bay as the review panel indicated that this dimension would be pre-established by architectural considerations. The design procedure focused on current applicable code provisions paired with these recommended parameters.

The design space for this study is the core walls of low to mid-rise (8–22 story) commercial buildings. The core walls are C-PSW/CF, and they are coupled using filled composite members (also known as concrete filled tubes). This design space is broken down into performance groups for the FEMA P695 study. Basic configuration, design load level, and structure period differentiate these performance groups. In this study, two structural configurations, under two seismic load levels were evaluated. These parameters correspond to 4 performance groups (PG) with up to 16 archetypes designed and analyzed. A summary of the performance groups is presented in Table 1.

The overall CC-PSW/CF archetypes are presented in Fig. 1a. The two structural configurations are coupled and uncoupled planar walls (Type I) and two coupled C-shaped walls (Type II) as shown in Fig. 1b. The typical coupling beam cross–section is shown in Fig. 1c. The maximum considered seismic demand for this system was seismic design category D. Both the maximum (D_{max} for which design spectral accelerations are $S_{DS} = 1.0\ g$ and $S_{D1} = 0.6\ g$) and minimum (D_{min} for which design spectral accelerations are $S_{DS} = 0.5\ g$ and $S_{D1} = 0.2\ g$) seismic design parameters were evaluated per the FEMA P695 procedure. The height of the structure influenced both the period and the wall configuration of the archetypes.

Initial archetype structures were designed by sizing walls and coupling beams based on the initial design parameters. These initial designs were then revised based on the results from design checks including maximum inter-story drift ratio, shear and flexural capacities, and plate slenderness ratio. The final design parameters were:

- Coupling beam aspect ratio (L_{beam}/d): 3, 4, or 5, where L_{beam} and d are the length and the depth of coupling beams.
- Story Height: First story was set to 17ft. (5182 mm) and other stories were 14ft. (4267 mm). These values were chosen based on the recommendation of the Peer Review Panel for story heights of typical mid-rise structures.
- Seismic weight: the seismic weight was calculated based on a floor load of 120psf (5.75 kPa) considering steel framing (12psf or 0.58 kPa) and superimposed dead load (15psf or 0.72 kPa), 2.5in. (63.5 mm) normal concrete slab on 3in. (76 mm) steel desk which is equal to 50psf (2.4 kPa), and weights of curtain wall (15psf or 0.72 kPa) and partitions (15psf or 0.72 kPa)
- The coupled wall length was set to 30ft. (9144 mm)
- Floor dimensions were chosen as 120ft.x200ft. (36,576 mm × 60,960 mm)
- The base shear amplification factor was selected as 4 based on recommendation of the Peer Review Panel. This factor amplifies the analysis base shear to account for higher mode effects, employing a similar approach as ACI318-19 uses for calculating the shear demand for coupled concrete shear walls. It should be noted that the shear strength of the walls was not a controlling limit state for any archetype structure due to the high shear strength of the section.

As this system is relatively new in its use as a seismic force resisting system, limited design procedures had been developed; therefore, a detailed design procedure was written. This design methodology sized coupling beams to resist seismic demand levels and wall elements to resist capacity limited seismic loads. This procedure ensured that the overall system behavior was governed by strong wall-weak coupling beam behavior. This capacity-based design philosophy for coupled C-PSW/CF systems is detailed further in Broberg et al. [7]. Establishing this design methodology ensured consistent archetype designs that met relevant code provisions and outlined design checks performed outside of currently existing code provisions to enforce the desired behavior. In general, the procedure followed the following steps: (1) Gather predetermined information (i.e. floor dimensions and core wall dimensions specified by the architect); (2) Perform Equivalent Lateral Force

Table 2
8- and 12-story archetypes. (Note: 1 in. = 25.4 mm; 1ft = 0.3048 m; 1sq in. = 645.2 mm^2; 1 in^4 = 416231 mm^4; 1 psi = 0.0069 MPa; 1 ksi = 6.9 MPa).

Case	No. Stories	L/d	Cs	Coupled Wall Length, in	Wall Thickness, t_{sc}, in	Plate Thickness, t_p, in	CB Length, in	CB Section, in	Uncoupled Wall Length, in	Performance Group
PG-1A		3		144	20	9/16	72	20x24x 3/8(t_f), 3/8(t_w)	252	1
PG-1B	8	4	0.076	132	24	9/16	96	24x24x 1/2(t_f), 3/8(t_w)	240	1
PG-1C		5		120	24	5/8	120	24x24x 1/2(t_f), 3/8(t_w)	240	1
PG-2B	8	4	0.024	144	10	3/16	72	10x18x 3/16(t_f), 1/4(t_w)	240	2
PG-1D		3		204	18	9/16	72	18x24x 5/16(t_f), 3/8(t_w)	348	1
PG-1E	12	4	0.057	192	22	9/16	96	22x24x 7/16(t_f), 3/8(t_w)	336	1
PG-1F		5		180	24	9/16	120	24x24x 1/2(t_f), 3/8(t_w)	324	1
PG-2E	12	4	0.017	204	8	3/16	72	8x18x 3/16(t_f), 1/4(t_w)	336	2

Table 3
18- and 22-story archetypes. (Note: 1 in. = 25.4 mm; 1ft = 0.3048 m; 1sq in. = 645.2 mm^2; 1 in^4 = 416231 mm^4; 1 psi = 0.0069 MPa; 1 ksi = 6.9 MPa).

Case	No. Stories	L/d	Cs	C wall depth, in (h_f)	C wall width, in (h_w)	$t_{sc.w}$, in	$t_{sc.f}$, in	$t_{p.bot}$, in	$t_{p.top}$, in	CB Length, in	CB Section, in	Performance Group
PG-3A		3		360	180	18	14	1/2	5/16	72	18x24x 5/16(t_f), 3/8(t_w)	3
PG-3B	18	4	0.042	360	168	24	14	1/2	5/16	96	24x24x 7/16(t_f), 3/8(t_w)	3
PG-3C		5		360	156	26	16	9/16	5/16	120	26x24x 1/2(t_f), 3/8(t_w)	3
PG-4B	18	4	0.014	360	162	12	12	3/16	3/16	72	12x18x 1/4(t_f), 1/4(t_w)	4
PG-3D		3		360	204	20	14	1/2	3/8	72	20x24x 3/8(t_f), 3/8(t_w)	3
PG-3E	22	4	0.036	360	192	24	14	1/2	3/8	96	24x24x 7/16(t_f), 3/8(t_w)	3
PG-3F		5		360	180	28	16	9/16	3/8	120	28x24x 9/16(t_f), 3/8(t_w)	3
PG-4E	22	4	0.012	360	162	14	10	3/16	3/16	72	14x18x 1/4(t_f), 1/4(t_w)	4

Analysis as defined in ASCE 7; (3) Choose preliminary dimensions for wall and coupling beam components; (4) Perform structural analysis; (5) Perform all design checks including strength, drift, and slenderness; (6) Redesign as necessary. For the taller structures, the steel plate thickness was reduced halfway up the structure in line with optimization typically performed in tall buildings. Additional optimization such as varying the plate thickness for all structures, reducing the coupling beam size, or decreasing the wall thickness was not performed. Although these design choices could have reduced the size of upper story members, they have limited impact on the seismic performance as the plastic hinge region of the walls has the largest effect on drift ratio. An example archetype designed explicitly using this procedure is provided in Appendix C of the Charles Pankow Foundation (CPF) report by Bruneau et al. [8]. As a result of this design procedure, properties of the archetypes selected for the FEMA P695 study are listed in Tables 2 and 3.

4. Nonlinear models

Two different modeling approaches were adopted for the two IDA analyses to be conducted in parallel as part of this study [11]. In the first

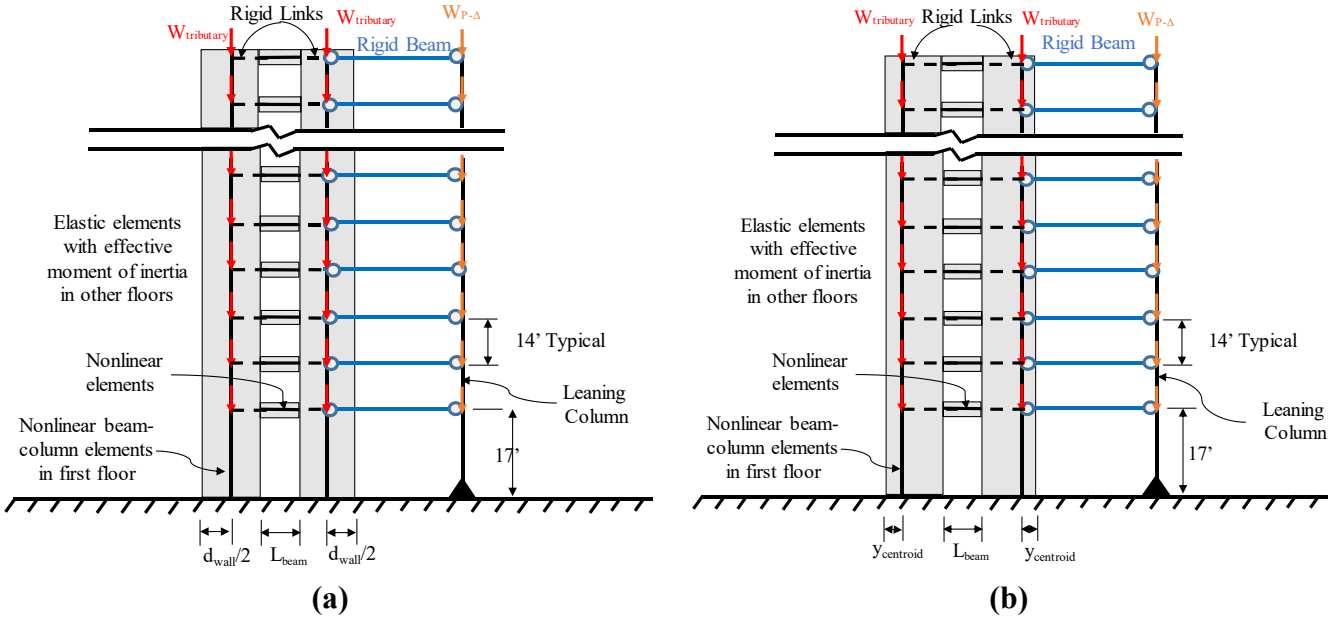

Fig. 2. Nonlinear model for collapse simulation for (a) coupled planar C-PSW/CF wall system and (b) coupled C-shaped C-PSW/CF wall system.

approach, walls and coupling beams were modelled using distributed plasticity based fiber elements (i.e., distributed plasticity model) with properties obtained from coupon test results and unconfined concrete strength. In the second approach, the walls were modelled with fiber-hinge elements having effective stress–strain curve obtained from Abaqus models [16], and the coupling beams were modelled with concentrated plastic hinge elements at their ends using a Modified Ibarra-Medina-Krawinkler Deterioration Model with Pinched Hysteretic Response (MIMKD Model) [10]. As mentioned before, the archetypes consist of walls and coupling beams. Planar and C-shaped composite wall configurations were considered, both having the same type of coupling beams, namely concrete filled rectangular steel tubes. Calibration and verification of the material model parameters and element sizes for these individual components of the CC–PSW/CF system has been addressed in a previous publication [11]. Building on the results reported in there, focus below is on how all of the components were assembled together in the two nonlinear modeling approaches used.

4.1. Distributed plasticity models

Fig. 2a and 2b show two-dimensional nonlinear models for the collapse simulation of coupled planar CC–PSW/CF and coupled C-Shaped CC-PSW/CF archetypes. All deterioration material models, element types, and size for each component of the CC-PSW/CF system, as well as

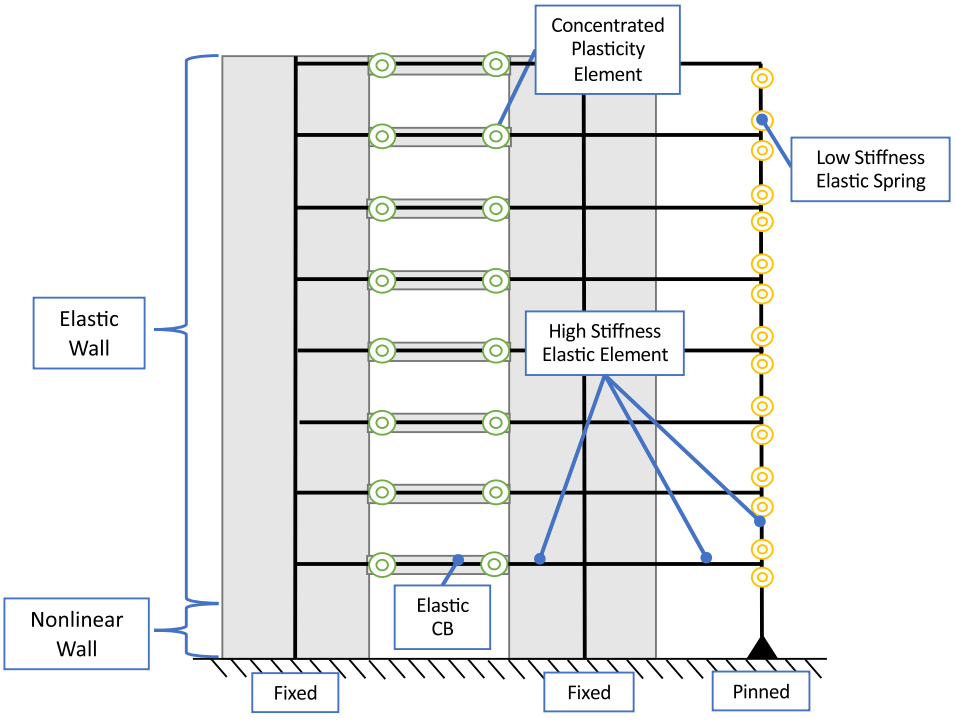

Fig. 3. Nonlinear model for collapse simulation for concentrated plasticity model.

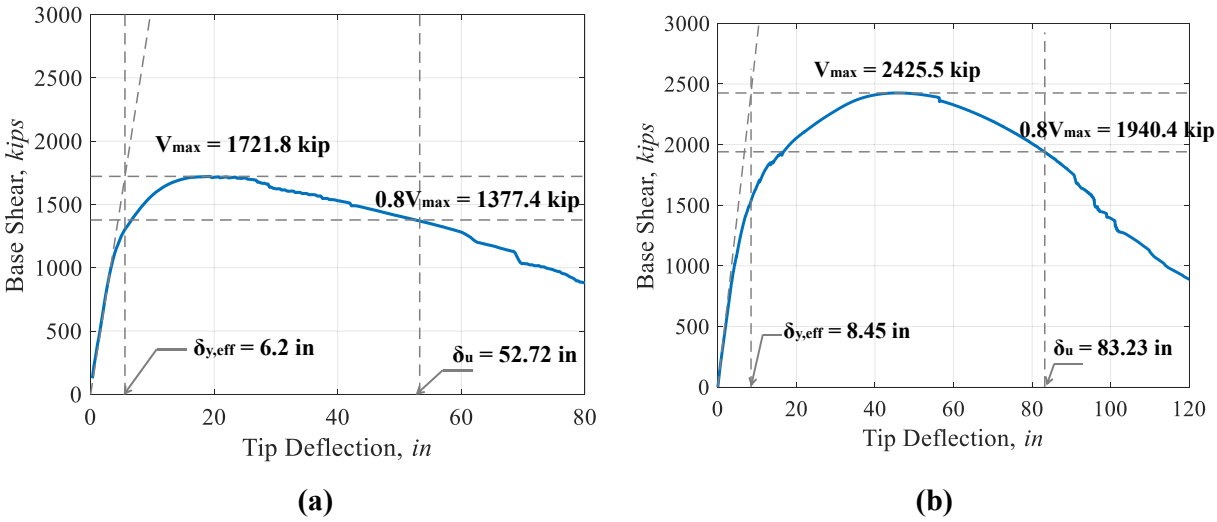

Fig. 4. Monotonic Pushover Analysis results for: a) PG-1C, and; b) PG-3C.

their calibration to test data, are presented in Kizilarslan et al. [11]. For walls, the nonlinear beam column elements were only assigned to the first floor of the walls and the rest of the floors were modeled using elastic beam-column elements having effective stiffness per AISC341 Equation I2-12 [1], whereas the coupling beams were modeled using only nonlinear beam column elements. The nonlinear elements were assigned to the centroid of the cross–section of composite walls as they were calibrated. Note that only half of the building was modeled, due to symmetry. For analyses purpose, half of C-shaped wall were modeled (but results are presented for full building later). Leaning columns were also added to the structural model to capture the P-Δ effects in each given story due to gravity loads that are not located on the CC-PSW/CF system itself (1440 kips (6405 kN)). They were modeled using elastic beam-column elements. Moment of inertia and cross section area of the elastic beam-column elements should be multiplied to represent the number of leaning columns assumed to exist in the archetype structure. Since there was no definitive information on the number of leaning columns in the archetype design, these values were chosen to provide insignificant flexural stiffness. Tributary loads coming to the C-PSW/CF walls (72 kips (320 kN) per floor for planar walls and 144 kips (640 kN) for C-Shaped walls) were applied to the wall at each floor. Rigid links were assigned between the C-PSW/CF wall center of gravity and the point where the coupling beams frame into the walls, and rigid beams were used to connect the leaning column and C-PSW/CF wall at every floor (these rigid beams were modeled using truss elements with a cross section area increased to 100 times the elastic area of the coupling beams. No seismic mass was assigned to the leaning column; seismic masses were applied to the C-PSW/CF walls and distributed equally to its left and right joints at every story. In the nonlinear time history analyses of the archetypes, Rayleigh damping was used, with a value of 5% damping specified for the first and second periods of vibration. The sensitivity of results to other damping ratios was also considered, as presented later.

4.2. Concentrated plasticity models

Fig. 3 shows the two-dimensional nonlinear models developed using distributed plasticity based fiber elements for the composite walls and concentrated plasticity based hinge models for the coupling beams. These models were used for the collapse simulation of coupled planar CC-PSW/CF and coupled C-Shaped CC-PSW/CF archetypes. The material models, element types, and component benchmarking are detailed in Kizilarslan et al. [11] and Broberg et al. [6]. For the wall, nonlinear beam column elements extended to the depth of the wall. This modeling choice is consistent with experimental results from Shafaei et al. [14] showing that yielding was limited to a height roughly equivalent to the depth of the wall. Above the nonlinear beam elements were elastic beam-column elements having an effective stiffness per AISC341 Equation I2-12 [1]. All wall elements were located at the geometric centroid of the wall sections.

The coupling beams were modelled with concentrated plasticity hinge elements at the ends connected with elastic beam elements. The concentrated plasticity hinges are zero length element representing the behavior of plastic hinges formed at the end of the coupling beams. Properties for these plastic hinge elements were calibrated to a distributed plasticity model of the coupling beam performance. This modeling choice was made because the concentrated plasticity element can be computationally more efficient than benchmarked distributed plasticity models. The coupling beam elements were connected to the wall elements using high stiffness elements.

The P-Δ effects were modelled using elastic beam-column elements with minimal stiffness. The gravity load from the system (1440 kips) was assigned to this leaning column. High stiffness elements connected the leaning column to the coupled wall system. Mass was distributed equally to each wall and lumped at the story level. No tributary load was applied to the coupled walls. The tributary load is much smaller than the wall capacity (and the balance point for the individual walls) so this choice has limited implications. For the time history analysis, 5% Rayleigh damping was applied for the first and second structural periods.

5. FEMA P695 study

5.1. Distributed plasticity model

Nonlinear pushover analysis was conducted, in compliance with the approach prescribed by the FEMA P695 methodology to estimate the overstrength (Ω_o) and period-based ductility (μ_T) factors for all archetypes. The overstrength (Ω_o) factor were obtained by dividing the maximum base shear obtained from the static pushover curve by the base shear for which archetypes were designed, as indicated in Eq. (1). In order to determine the period-based ductility (μ_T) factor, ultimate top floor displacements are divided by effective yield displacement (Eq. (2)). The effective yield displacement ($\delta_{y,eff}$) was taken as the displacement corresponding to the intersection of a line tangent to the initial slope of the resulting pushover curve and a horizontal line set at the level of the maximum base shear obtained from this nonlinear pushover analysis, V_{max}. The displacement obtained at $0.8V_{max}$ on the descending branch (i.e., post-peak) of the pushover curve was taken for the ultimate top floor

Table 4
Summary of Performance Evaluation for CC-PSW/CF Archetypes with Distributed Plasticity Model. (Note: 1 in. = 25.4 mm; 1ft = 0.3048 m; 1sq in. = 645.2 mm2; 1 in4 = 416231 mm4; 1 psi = 0.0069 MPa; 1 ksi = 6.9 MPa).

Performance Group	Archetype	Pushover Results						IDA Results			Performance Evaluation				
		V_d, kips	V_{max}, kips	$\delta_{y,eff}$, in	δ_u, in	Ω_o	μ_T	$\hat{S}_{CT}$, g	S_{MT}, g	CMR	SSF[a]	ACMR	Pass/Fail	$ACMR_{ave}$	Pass/Fail
1	PG-1A	879	1953	4.16	29.26	2.22	7.03	3.33	0.90	3.70	1.25	4.63	Pass	4.27	Pass
	PG-1B	879	1877	4.33	33.95	2.14	7.84	2.61	0.86	3.03	1.26	3.82	Pass		
	PG-1C	879	1722	6.20	52.72	1.96	8.50	2.08	0.75	2.77	1.28	3.55	Pass		
	PG-1D	979	2284	6.20	36.53	2.33	5.89	1.99	0.642	3.10	1.306	4.05	Pass		
	PG-1E	979	2279	6.40	41.86	2.33	6.54	2.42	0.64	3.78	1.31	4.95	Pass		
	PG-1F	979	2105	6.80	46.78	2.15	6.88	2.10	0.60	3.50	1.32	4.62	Pass		
2	PG-2B	273	560	2.79	29.81	2.05	10.68	0.69	0.1765	3.91	1.21	4.73	Pass	5.22	Pass
	PG-2E	305	650	4.49	35.30	2.13	7.86	0.59	0.125	4.72	1.21	5.71	Pass		
3	PG-3A	1088	2388	7.51	51.96	2.19	6.92	1.86	0.45	4.13	1.32	5.45	Pass	6.58	Pass
	PG-3B	1088	2586	8.41	68.48	2.38	8.14	1.69	0.44	3.84	1.32	5.07	Pass		
	PG-3C	1088	2426	8.45	83.23	2.23	9.85	1.51	0.42	3.60	1.32	4.75	Pass		
	PG-3D	1146	2927	12.56	66.43	2.55	5.29	1.78	0.36	4.94	1.32	6.52	Pass		
	PG-3E	1146	2642	13.42	79.73	2.31	5.94	1.53	0.23	6.65	1.32	8.78	Pass		
	PG-3F	1146	2727	12.55	99.20	2.38	7.90	1.55	0.23	6.74	1.32	8.90	Pass		
4	PG-4B	338	749	5.19	53.00	2.22	10.21	0.52	0.07	7.43	1.21	8.99	Pass	8.49	Pass
	PG-4E	356	672	9.30	60.16	1.89	6.47	0.31	0.047	6.60	1.21	7.99	Pass		

a SSF obtained from FEMA P695 (2009) table for given T and μT.
Note: Acceptance criteria: ACMR ≥ ACMR20% = 1.56 (from Table 7-3 in FEMA P695 (2009) based on βTOT) for individual comparison.
ACMRave ≥ ACMR10% = 1.96 for average of performance group comparison, otherwise fail.

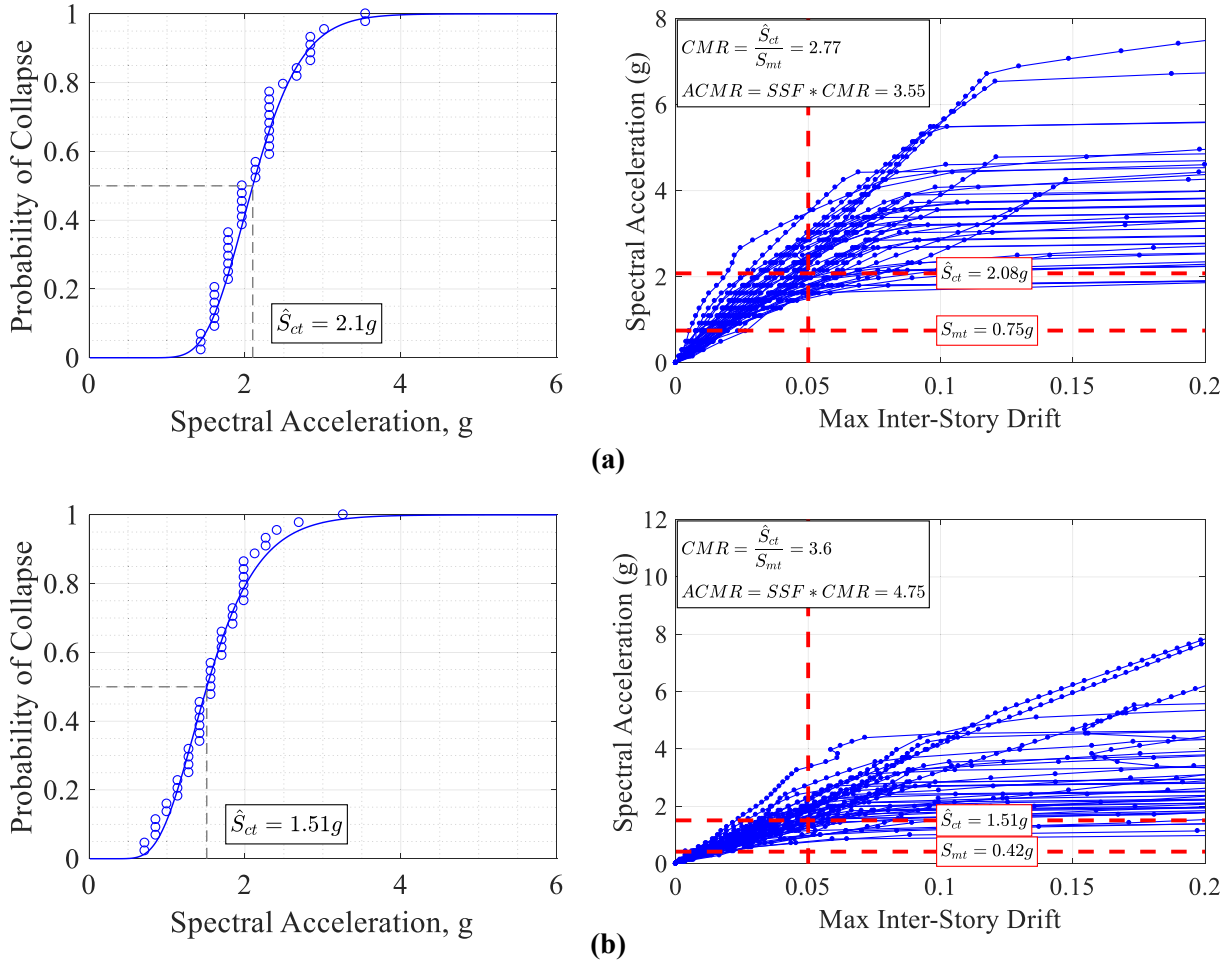

Fig. 5. Incremental Dynamic Analysis results for: a) PG-1C, and; b) PG-3C.

displacement (δ_u). The nonlinear pushover results of PG-1C and PG-3C are presented in Fig. 4a and 4b, respectively. The results of these pushover analyses for all archetypes are tabulated in Table 4.

$$\Omega_o = \frac{V_{max}}{V_{design}} \tag{1}$$

$$\mu_T = \frac{\delta_u}{\delta_{y,eff}} \tag{2}$$

Incremental dynamic analysis (IDA) consists of a series of successive time history analyses performed for a given structural model, for which the intensity of ground motions specified is gradually scaled up from low to high magnitude until collapse is observed in the structure. Theoretically, there is no unique rule for choosing intensity increments for IDA. In other words, any incremental scheme of ground motion intensity can be selected. In this research project, the default 44 far-field ground motions specified by FEMA P695 were used and the IDA started with an analysis using half of the actual un-scaled recorded ground motions, followed by one using the actual un-scaled record itself. The subsequent increments for which all ground motions were scaled were such that the median spectral acceleration of the 44 ground motions (at the fundamental period of a given archetype being analyzed) matched that at the Design Basis Earthquake (DBE) and at the Maximum Considered Earthquake (MCE) spectral acceleration levels, respectively. From there, each motion was gradually scaled up in steps equal to four-tenth, six–tenth, one, and one–and–half of the MCE level (i.e., $0.4S_{a\text{-}MCE}$, $0.6S_{a\text{-}MCE}$, $1.0S_{a\text{-}MCE}$, and $1.5S_{a\text{-}MCE}$) for the 8-, 12-, 18- and 22-story archetypes, respectively, up to the intensity that caused structural collapse for each individual ground motion. The balance sought was to limit the number of analyses to a manageable number while maintaining sufficient accuracy in determining the collapse intensity level. For comparison, when increments equal instead to one-tenth of the median spectra value were used beyond the MCE level (which was performed with selected ground motions), the obtained resulted were found to be comparable but it required more than a hundred nonlinear analysis before reaching collapse intensity, which was deemed to be too computationally intensive for a relatively small accuracy gain in the determination of the intensity at collapse. Such increased accuracy also became a moot point once it was realized that calculation of the collapse margin ratio would be performed in all cases at 5% drift (i.e., much smaller drifts than at the points of actual collapse), as described below.

In a typical IDA curve, when the IM (intensity measure) vs DM (damage measure) curves become a nearly flat line upon increasing values of IM, it is an indication of structural collapse (or dynamic instability), because in this case, a slight increase in ground motion intensity from that in the previous IDA step causes extreme increases in lateral deformations of the structure under consideration. However, in most cases, for the types of structure considered here, collapse by this definition was often observed to occur at extreme drifts of nearly 10% (or more in some cases). As such, other considerations were taken into account to define "collapse" from a practical perspective. Therefore, in addition to the "actual collapse" observed from the IDA, a semi-arbitrary practical drift limit was also used here as a definition of collapse. Recognizing that real buildings would suffer an extensive amount of non-structural damage if developing 5% drift during seismic response, even if not experiencing global collapse proper, for the IDA conducted here as part of this FEMA P695 study, when actual collapse occurred at drifts larger than 5%, the Collapse Margin Ratio (CMR) was calculated based on response values obtained at 5% drift for each archetype.

Fig. 5a and 5b present IDA results (right) obtained for PG-1C and PG-3C archetypes considered and their corresponding fragility curves (left) developed based on the spectral accelerations at 5% maximum inter-story drifts (i.e., using IDA point closest to 5% drift). For each archetype, the median collapse spectral acceleration intensity at 5% maximum inter-story drift (defined to be the limiting collapse definition), $\hat{S}_{CT}$, is the spectral acceleration intensities that corresponded to a 50% probability of collapse at 5% maximum inter-story drift on the fragility curve. These curves were obtained by fitting a lognormal distribution through the "collapse" data points. Note that for a lognormal distribution [3,5,9], the median value of the collapse data points as $\hat{S}_{CT}$ is used here instead of the average (arithmetic mean).

The median collapse spectral acceleration intensity, $\hat{S}_{CT}$ and the median spectral acceleration, S_{MT} of all archetypes are compiled in Table 4. From these IDA results, the collapse margin ratio (CMR) was calculated as the ratio between $\hat{S}_{CT}$ and S_{MT}, per Eq. (3).

$$CMR = \frac{\widehat{S}_{CT}}{S_{MT}} \tag{3}$$

Per FEMA P695, the CMR value obtained from the IDA were then adjusted to take into account the frequency content of the selected ground motion records (i.e., the effect of spectral shape). The spectral shape factor (SSF) values that are used to modify the CMR to the adjusted collapse margin ratio (ACMR) are a function of the archetype fundamental period, the applicable Seismic Design Category (SDC) and period-based ductility (μ_T) attained from nonlinear pushover analysis. The period-based ductility (μ_T) was conservatively taken as 3 for all archetypes, based on observed behavior in experimentally obtained cyclic hysteretic curves, even though the nonlinear pushover analysis of archetypes proved that the ductility is more than 3 for all archetypes. The value of SSF are obtained from Tables 7-1a and 7-1b (depending on SDC) in the FEMA P695 document for both archetypes. Accordingly, the ACMR are obtained by multiplying the CMR by the SSF value as in Eq. (4).

As such, total system collapse uncertainty (β_{TOT}) is required in order to calculate the acceptable ACMR value. The value of β_{TOT} is obtained by combining uncertainty factors related to record- to-record (β_{RTR}), design requirements (β_{DR}), test data (β_{TD}), and nonlinear modeling (β_{MDL}). For the selected ground motions used in the FEMA P695 methodology, a constant value of β_{RTR} equal to 0.4 is used, given that period-based ductility is larger than or equal to 3 ($\mu_T \geq 3$). With respect to the other three uncertainty factors (β_{DR}, β_{TD}, and β_{MDL}), these values were taken as equal to 0.2, corresponding to the "good" rating (i.e., β_{DR}, β_{TD}, and $\beta_{MDL} = 0.2$), which is justified both based on the quality of the information available and past practice and similar studies [12]. The corresponding total system uncertainty calculated using Eq. (5) is 0.529. The acceptable ACMR for 10% and 20% collapse probability under MCE ground motions (i.e., $ACMR_{10\%}$ and $ACMR_{20\%}$) for β_{TOT} of 0.529 are 1.96 and 1.56 from Table 7-3 in FEMA P695 document, respectively.

The FEMA P695 methodology specifies that $ACMR_{20\%}$ and $ACMR_{10\%}$ are the acceptable threshold values to evaluate performance of individual archetype and average performance of several archetypes in one performance group, respectively. Hence, here, all individual archetypes passed the $ACMR_{20\%}$ performance requirement. Results in Table 4 show that for β_{TOT} of 0.529 and "good" rating, all individual 8-, 12-, 18- and 22-story archetypes are considerably above the $ACMR_{20\%}$ threshold. Likewise, average of ACMR values in a performance group also passed $ACMR_{10\%}$ threshold.

Note that even if all these values of uncertainties were actually be taken as "poor" here, rather than "good" (i.e., with β_{DR}, β_{TD}, and $\beta_{MDL} = 0.5$), the corresponding ACMR values (i.e., $ACMR_{10\%}$ and $ACMR_{20\%}$) calculated for the resulting β_{TOT} of 0.954 with "poor" rating would be 3.38 and 2.22, and the ACMR of the archetypes considered would still have been found to be satisfactory.

Results from the collapse performance evaluations of the 8-, 12-, 18- and 22-Story archetypes indicate that the initial R factor of 8 used to design the archetypes considered is adequate. Results also indicate that the system over-strength factor (Ω_o) could be specified as 2.34 (which is the largest average value of the calculated archetype overstrength in all performance groups (2.19 for PG-1, 2.26 for PG-2, 2.34 for PG-3, and 2.06 for PG-4)) and that the deflection amplification factor (C_d) could be taken as equal to 5.5, which is the value for which all archetypes were

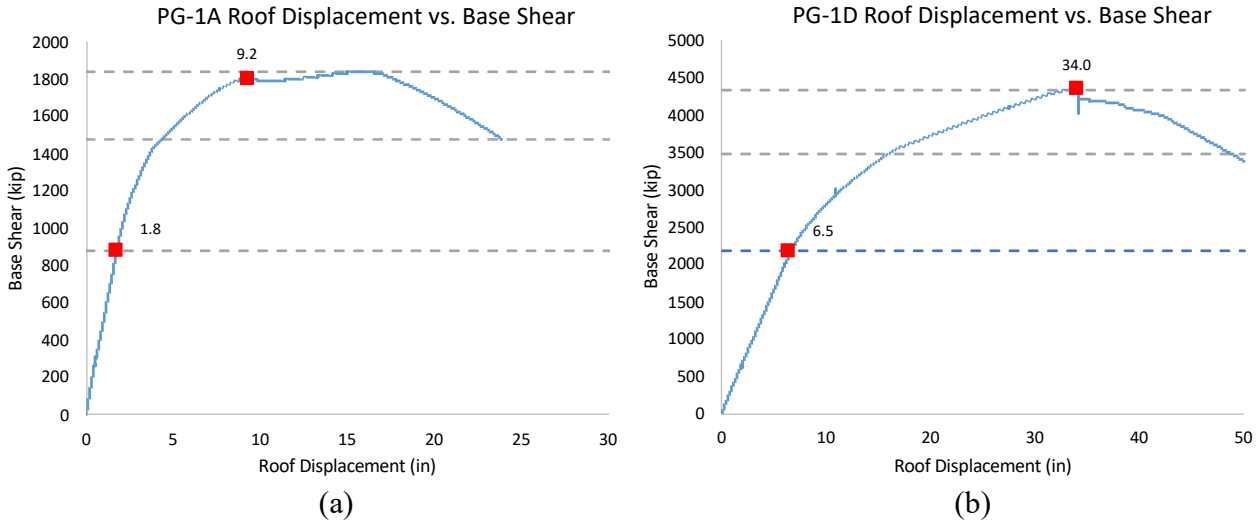

Fig. 6. Monotonic Pushover Analysis results for: a) PG-1C, and; b) PG-3C.

Table 5
Summary of performance evaluation for CC-PSW/CF archetypes with concentrated plasticity model.

Performance Group	Archetype	Pushover Results						IDA Results			Performance Evaluation				
		V_d, kips	V_{max}, kips	$\delta_{y,eff}$, in	δ_u, in	Ω_o	μ_T	$\hat{S}_{CT}$, g	S_{MT}, g	CMR	SSF[a]	ACMR	Pass/Fail	$ACMR_{ave}$	Pass/Fail
1	PG-1A	879	1843	2.4	23.9	2.1	10.0	2.24	0.87	2.57	1.26	3.24	Pass	3.87	Pass
	PG-1B	879	1797	2.5	29.9	2.0	12.0	2.05	0.84	2.44	1.27	3.10	Pass		
	PG-1C	879	1534	2.7	33.9	2.1	12.7	1.96	0.75	2.61	1.28	3.35	Pass		
	PG-1D	979	2244	3.5	26.3	2.3	7.5	2.32	0.65	3.57	1.31	4.68	Pass		
	PG-1E	979	2208	3.3	34.2	2.3	10.3	2.27	0.66	3.44	1.31	4.51	Pass		
	PG-1F	979	2023	3.6	40.2	2.1	11.3	2.02	0.61	3.31	1.32	4.37	Pass		
2	PG-2B	273	574	1.9	20.1	1.7	10.8	0.92	0.18	5.11	1.21	6.18	Pass	6.70	Pass
	PG-2E	305	711	3.1	23.7	2.3	7.7	0.71	0.13	5.48	1.32	7.21	Pass		
3	PG-3A	1088	4346	7.8	32.0	2.0	4.1	0.76	0.34	2.21	1.32	2.95	Pass	2.60	Pass
	PG-3B	1088	4470	8.8	43.2	2.1	4.9	0.63	0.34	1.85	1.32	2.45	Pass		
	PG-3C	1088	4344	8.6	48.0	2.0	5.6	0.55	0.34	1.79	1.32	2.14	Pass		
	PG-3D	1146	4889	12.1	42.5	2.1	3.5	0.59	0.28	2.11	1.32	2.78	Pass		
	PG-3E	1146	4691	11.9	54.2	2.0	4.6	0.54	0.27	1.98	1.32	2.64	Pass		
	PG-3F	1146	4923	11.1	54.7	2.2	4.9	0.56	0.28	2.01	1.32	2.64	Pass		
4	PG-4B	338	711	6.7	32.1	2.3	4.8	0.28	0.08	3.55	1.21	4.24	Pass	4.24	Pass
	PG-4E	356	1858	11.7	40.2	2.6	3.4	0.21	0.06	3.73	1.21	4.24	Pass		

[a] SSF obtained from FEMA P695 (2009) table for given T and $\mu_T = 3.0$.
Note: Acceptance criteria: ACMR $\geq$ $ACMR_{20\%} = 1.56$ (from Table 7-3 in FEMA P695 (2009) based on β_{TOT}) for individual comparison.
$ACMR_{ave} \geq ACMR_{10\%} = 1.96$ for average of performance group comparison, otherwise fail.

designed.

$$ACMR = SSF(T, \mu_T) x CMR \tag{4}$$

$$\beta_{total} = \sqrt{\beta_{RTR}^2 + \beta_{DR}^2 + \beta_{TD}^2 + \beta_{MDL}^2} \tag{5}$$

5.2. Concentrated plasticity model

Similarly, nonlinear pushover and time-history analysis following the FEMA P695 methodology was performed for the concentrated plasticity model. Nonlinear pushover analysis was performed to estimate the overstrength (Ω_o) and period-based ductility (μ_T). These parameters were determined using the same procedure described previously. The pushover response for PG-1C and PG-3C are presented in Fig. 6. Results for all structures are shown in Table 5.

Incremental dynamic analysis was performed to determine the earthquake magnitude associated with failure. The same ground motions and procedure adopted for the distributed plasticity model was implemented to analyze the concentrated plasticity models. In addition to the procedure, the collapse definition of an inter-story drift equal to 5% and β_{TOT} were also applied to the concentrated plasticity model. This resulted in the incremental dynamic analysis response presented in Fig. 7 for PG-1C and PG-3C. Results for all structures are shown in Table 5.

Comparing the results in Tables 4 and 5 indicates that:

(i) For the planar wall archetype structures in performance group 1, the ACMR value for the models with concentrated plasticity (Table 5) are conservative.
(ii) For the planar wall archetype structures in performance group 2, the ACMR value for the models with distributed plasticity (Table 4) are slightly more conservative.
(iii) For the C-shaped wall archetype structures in performance groups 3 and 4, the ACMR values for the models with concentrated plasticity (Table 5) are more conservative.

These differences are attributed to the fundamental differences in

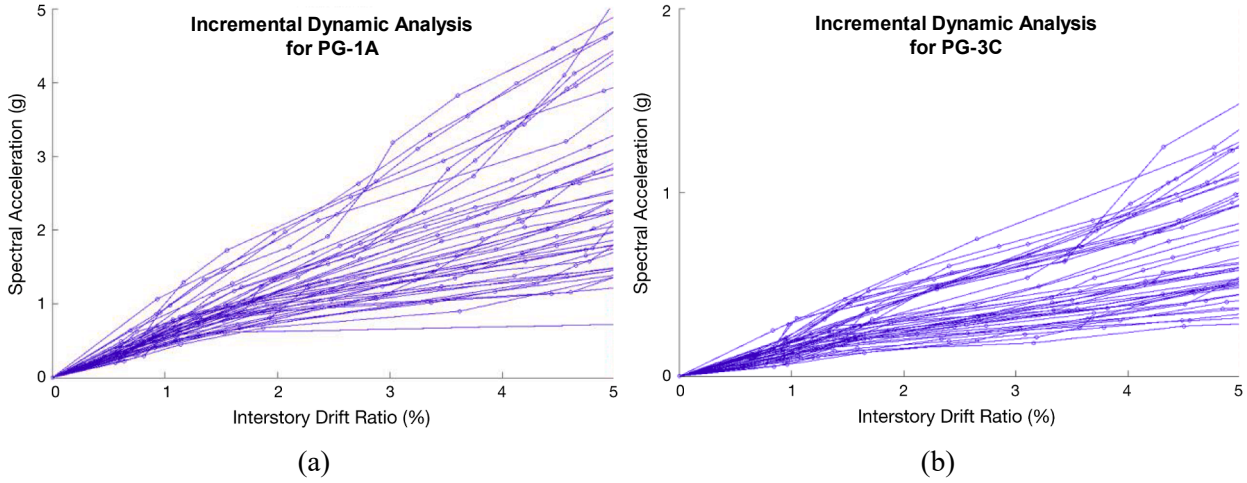

Fig. 7. Incremental Dynamic Analysis results for: a) PG-1C, and; b) PG-3C.

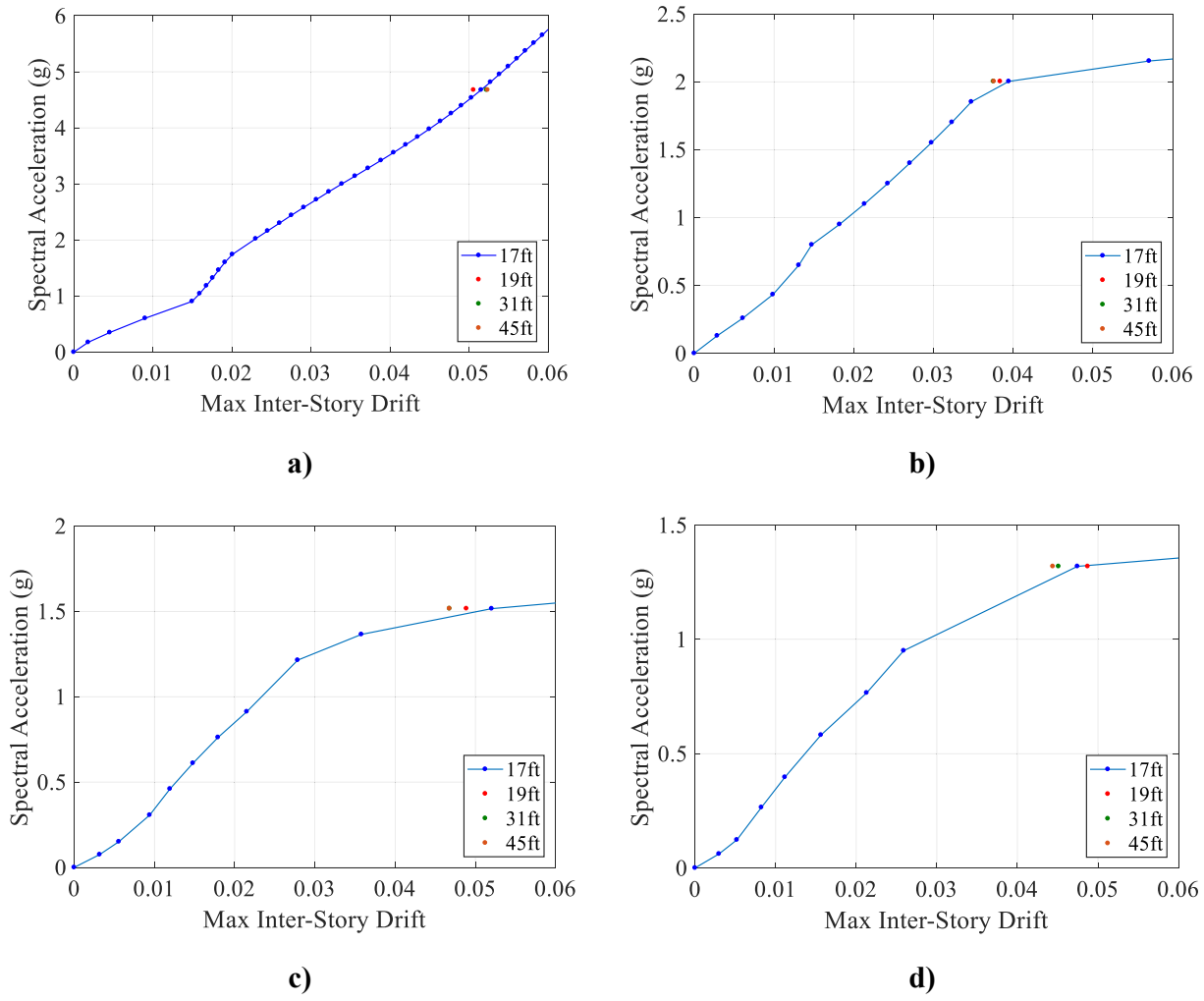

Fig. 8. Hinge length study done for: a) PG-1A, b) PG-1D, c) PG-3A, and; d) PG-3D.

modeling behavior, limit states, and local failure modes between the two modeling approaches. In particular, the coupling beams modeled using concentrated plasticity hinges followed pre-defined envelops of cyclic behavior and failure, and therefore could not account for the effects of cyclic loading history and plastic strain accumulation. The distributed plasticity models for coupling beams could explicitly account for the effects of cyclic loading history and plastic strain accumulation. Consequently, the concentrated plasticity hinge models are more conservative and estimate earlier onset of fracture failure in the coupling beams. This is evident by comparing the S_{ct} values between Tables 4 and 5, which are generally lower for the models with concentrated plasticity (Table 5). The S_{mt} values are quite comparable between Tables 4 and 5.

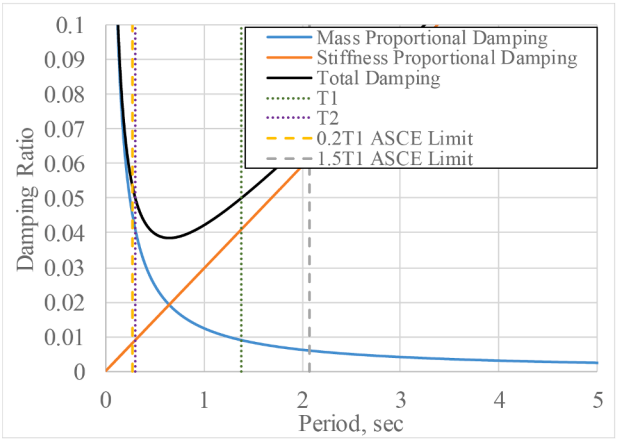

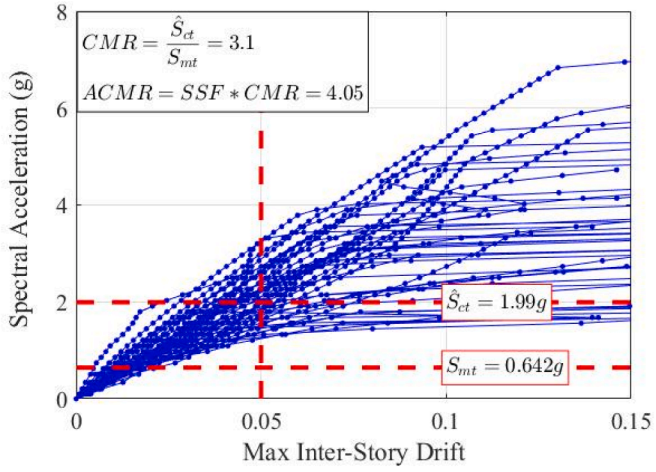

a)

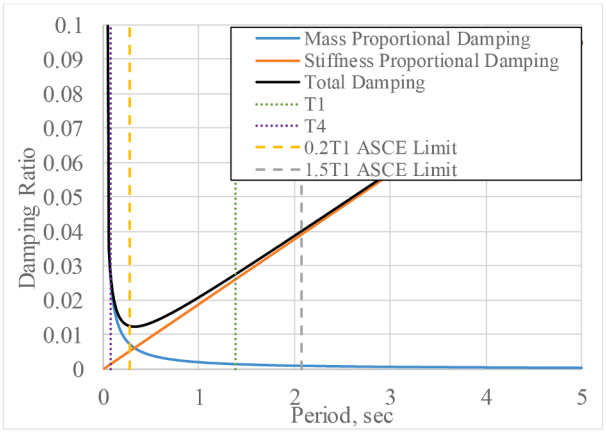

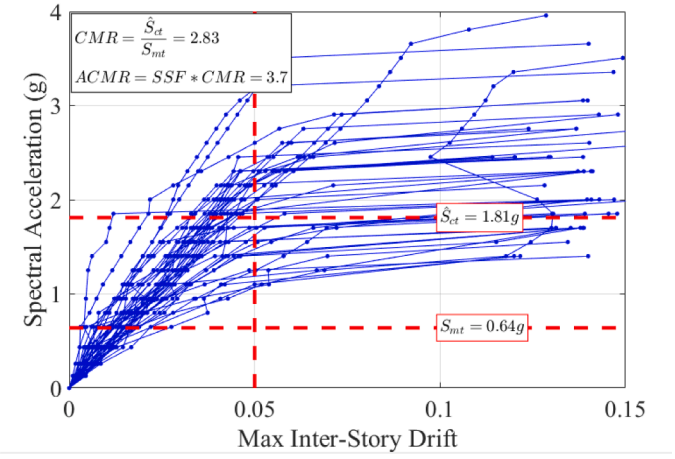

b)

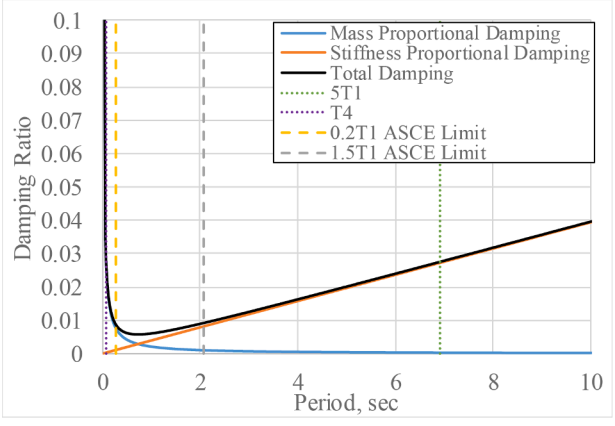

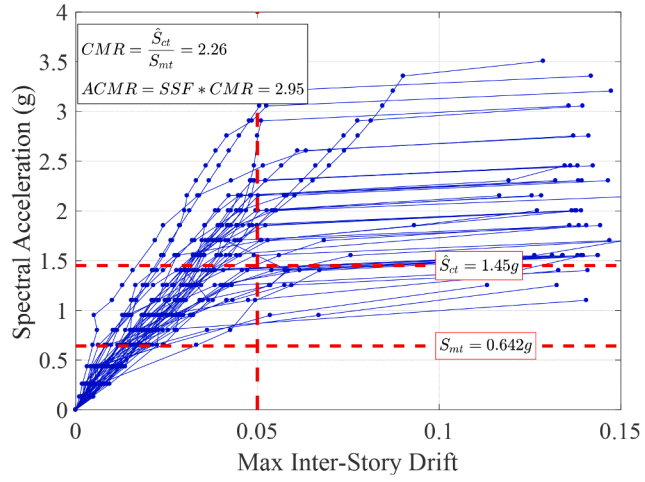

c)

Fig. 9. Results for PG-1D with Rayleigh Damping ratio set to: a) 5% at the 1st and 2nd periods, b) 2.75% at the 1st and 4th periods, and; c) 2.75% at 5 time the 1st period and 4th period.

Therefore, the differences in the CMR values (defined as the ratios of S_{ct} to S_{mt} values) and the subsequent ACMR values are directly attributed to the differences in the S_{ct} values, which can be attributed to the conservatism of the concentrated plasticity hinge models for the coupling beams.

6. Complementary studies

6.1. Plastic hinge length

It was mentioned previously that the nonlinear beam–column elements were only assigned to the first floor of the walls to model the plastic hinging of the walls. However, the plastic hinge length is physically defined by the distance from the point of maximum moment (at the base of the wall here) to the point along the height where the cross-section starts to yield. It was observed from pushover analysis of archetype models that this point of first yielding of the wall cross-sections can actually be up to the height of the third story. Therefore, a plastic hinge length study was performed for archetypes PG-1A, PG-1D, PG-3A, and PG-3D to investigate if IDA results were sensitive to the effect of using longer plastic hinge lengths. For this study, the region over which nonlinear elements were used was increased to 19ft. (or 5791 mm) (2ft. (609.6 mm) above 1st floor), 31ft. (9449 mm) (2nd floor), and 45ft. (13716 mm) (3rd floor) in the models of the chosen archetypes and analyses were run with the N-S component of the Superstition Hills (BICC090) earthquake at their corresponding spectral acceleration levels at 5% maximum interstory drift. Fig. 8 shows that increasing the plastic hinge length did not affect the IDA curve. For example, the maximum error observed in these plots is 6.4% in Fig. 8c.

6.2. Damping ratio study

In the nonlinear time history analyses of the archetypes, Rayleigh damping was used, with a value of 5% damping specified for the first and second periods of vibration. However, later, it was noticed that first and second modes of vibration contribute to only 80% of the total mass participation factor. It was further observed that in all of the archetypes, 90% of total mass participation factor contributing to the nonlinear analysis when the first four modes of vibration were considered, and additional analyses were therefore run with Rayleigh damping values of 5% anchored at the first and fourth periods of vibrations. In these subsequent analyses, the damping ratio was also reduced to a value based on the height of the structure, in accordance with the following equation from PEER TBI Section 4.2.7 [13]:

$$\xi_{critical} = \frac{0.36}{\sqrt{H}} \tag{6}$$

where H is the height of the structure in feet.

Therefore, for this sensitivity study of results to damping values, the PG-1D archetype was first selected because it was the tallest archetype of those having smallest ACMR. Fig. 9a shows the IDA results obtained for the PG-1D archetype with a 5% damping ratio anchored at the first and second periods of vibration. Then, the same archetype was run with the 2.75% damping ratio value, obtained from Eq. (6), anchored at the first and fourth periods of vibration. The resulting adjusted collapse margin ratio (ACMR) decreased by 8.6% (Fig. 9b).

After further studying the behavior of these lateral loading resisting systems, it was observed that the composite walls are behaving individually at a much larger period of vibration after all coupling beams have fractured, which typically happened at drift of 5% or larger (the walls would also eventually develop a rocking behavior once fully fractured [8]. As a result, the period of the system elongates significantly during that later stage of response. In order to prevent overdamping of the structural system when it shifts to those higher periods of vibration, it was decided to also perform analyses with 2.75% damping ratio anchored at a period equal to five times the first period and at the fourth period of vibration. Using such an extreme anchoring period resulted in a damping ratio of less than 1% at the first period of vibration which contributes to 80% of the total modal participation factor (as listed in Table 6). With this significantly less damped model, the ACMR of PG-1D decreased by 27.2%, from 4.05 to 2.95, compared to the IDA results initially obtained from 5% damping (Fig. 9c). However, note that even for these significantly less damped walls, the lower ACMR obtained were still sufficient to meet the FEMA P695 limits.

Table 6
Incremental dynamic analysis (IDA) results of PG-1C, PG-1D, PG-3C, and; PG-3D archetypes with reduced damping ratio (Units: kips, in, sec., g).

Parameter	PG-1C	PG-1D	PG-3C	PG-3D
S_{CT}	1.13	1.45	0.89	1.0
S_{MT}	0.75	0.642	0.42	0.36
First Period	1.192	1.382	2.14	2.49
Damping Ratios at First Period	0.88%	0.7%	0.596%	0.511%
CMR = S_{CT}/S_{MT}	1.51	2.26	2.12	2.78
ACMR	1.93	2.95	2.8	3.67

To ensure that other archetypes also meet the FEMA P695 ACMR limits when subjected to significantly lower damping, all the archetypes that were previously found to have the worst ACMR in their corresponding groups (i.e., PG-1C, PG-1D, PG-3C, and PG-3D) were re-analyzed with a lesser damping ratio, as calculated from Eq. (6) and anchored at five times the first period and at the fourth period of vibration. It was believed that if the worst ACMR value in a performance group was found to have an acceptable ACMR when considering this reduced damping, then the others would also be adequate. Fig. 10 shows the results of these additional IDA analyses for the selected archetypes. Table 6 summarizes these results for these selected archetypes for the various damping ratios considered. Among all selected archetypes, only PG-1C, with a 1.93 ACMR value, did not satisfy the $ACMR_{20\%}$ limit of 1.96. However, the difference between ACMR and $ACMR_{20\%}$ limit is marginal (namely, a 0.03 difference), and negligible considering that the anchored period (chosen to capture the period elongation after all coupling beam fracture) was taken as the extreme case of being at five times the first period of vibration. Therefore, all ACMR of the archetypes considered are considered to be satisfactory for this lower damping.

7. Summary and conclusions

Although Coupled Composite Plate Shear Walls—Concrete Filled (CC-PSW/CF) were intuitively understood to be more ductile and to have more redundancy than non-coupled composite plate shear walls, ASCE 7–16 does not differentiate between the two systems and does not assign them seismic design coefficients and factors (in Table 12.2-1 of ASCE 7–16). The FEMA P695 study presented here was conducted to substantiate the design coefficients and factors that should be used for such CC-PSW/CF structures. Adding this as a separate category in ASCE 7 Table 12.2-1 is important because modern buildings often have core-wall systems; many of these core walls could utilize the CC-PSW/CF.

A number of 8-story, 12-story, 18 story, and 22-story archetypes were designed, each considering 4 different coupled-walls properties, resulting in a total of 16 different archetypes. The archetypes were designed using an R value of 8 and C_d value of 5.5. The 8 and 12-story archetype structures used planar composite walls, while the 18 and 22 story archetype structures used C-shaped walls. Non-linear time history dynamic analyses were performed as part of an IDA using two different sets of non-linear models.

Results from the FEMA P695 studies conducted using these IDA indicated that all archetypes reached collapse at drifts greater than 5%, but all collapse margin ratios established here were conservatively calculated based on results obtained at 5% drift (i.e., at less than actual collapse points). For all the archetypes considered, the lowest obtained calculated Adjusted Collapse Margin Ratios were respectively 3.55,

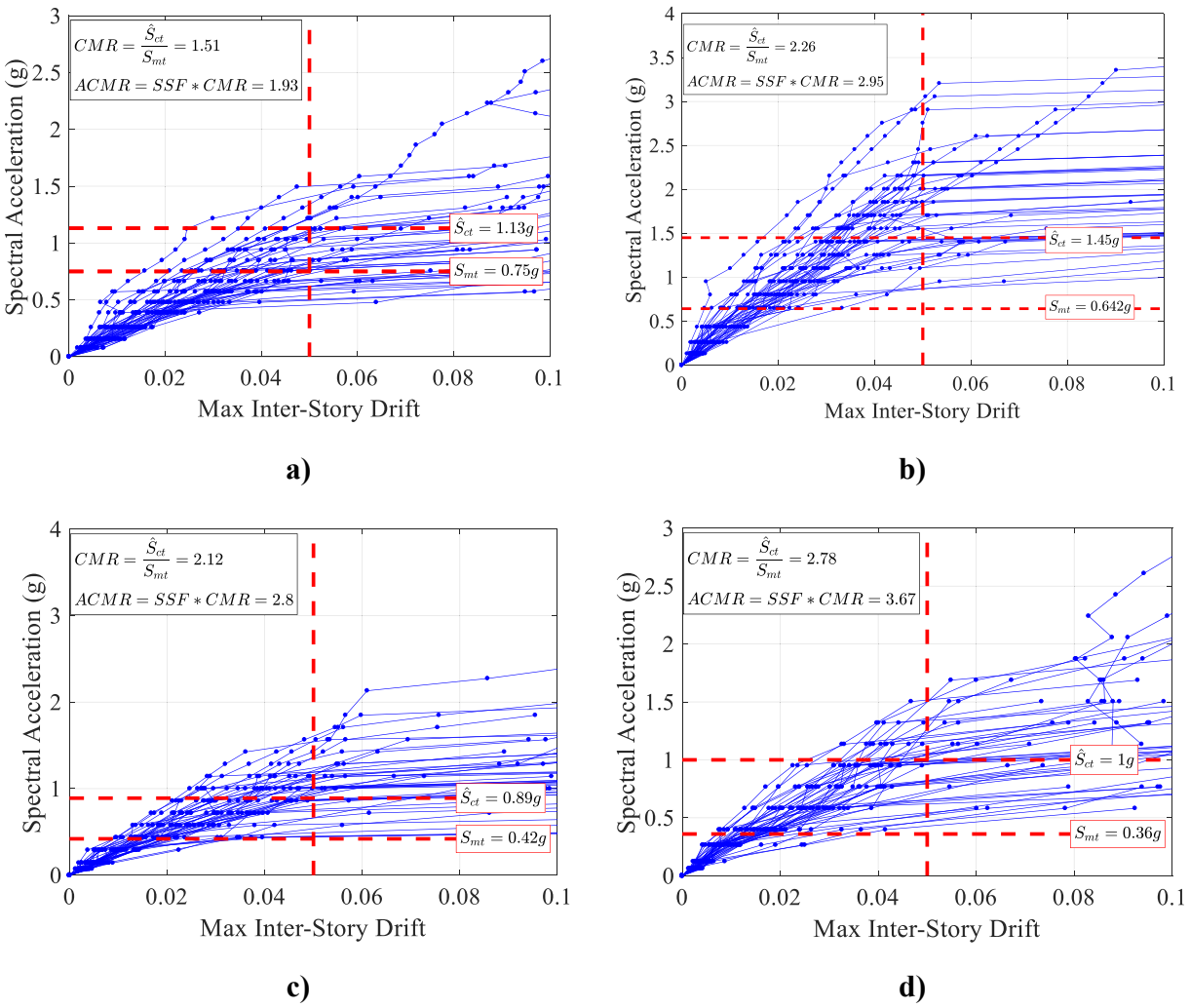

Fig. 10. Reduced damping study done for: a) PG-1C, b) PG-1D, c) PG-3C, and; d) PG-3D.

4.05, 4.75, and 6.52 for the 8, 12, 18, and 22 story archetypes for the IDA conducted with the first set of non-linear models; corresponding values of 3.10, 4.37, 2.14, and 2.64 were respectively obtained for the 8, and 12, 18, and 22 story archetypes for the IDA conducted with the second set of non-linear models. All ACMR were calculated for a $\mu_T = 3.0$. These ACMR were compared with the acceptable adjusted collapse margin ratio values of 1.96 and 1.56 for $ACMR_{10\%}$ and $ACMR_{20\%}$. These values are obtained for a total system collapse uncertainty, β_{TOT}, calculated using a "good" rating for the design requirements related collapse uncertainty, test data related collapse uncertainty, and modelling related collapse uncertainty (incidentally, the ACMR would have been found acceptable even if the ratings had been "fair", or even mostly "poor"). Overstrength factor, Ω_o, for the archetypes were found to be on the order of 2.0 to 2.5, and the C_d for the archetypes were found to be 5.5. Complementary studies conducted to check the sensitivity of results to assumptions related to damping and yielding models confirmed the validity of this finding.

The findings from this study substantiated a set of proposed values for CC-PSW/CF for implementation in ASCE 7–22. Peer-review by the relevant ASCE Technical Committees have approved the findings from this research project, and the proposed new values will be in ASCE 7–22.

CRediT authorship contribution statement

Emre Kizilarslan: Validation, Investigation, Formal analysis, Data curation, Writing – original draft, Writing – review & editing, Visualization, Conceptualization. **Morgan Broberg:** Validation, Investigation, Formal analysis, Data curation, Writing – review & editing, Visualization, Conceptualization. **Soheil Shafaei:** Validation, Investigation, Formal analysis, Data curation, Writing – review & editing, Visualization, Conceptualization. **Amit H. Varma:** Supervision, Project administration, Writing – review & editing, Visualization, Conceptualization, Methodology, Funding acquisition. **Michel Bruneau:** Supervision, Project administration, Writing – original draft, Writing – review & editing, Visualization, Conceptualization, Methodology, Funding acquisition.

Declaration of Competing Interest

The authors declare that they have no known competing financial interests or personal relationships that could have appeared to influence the work reported in this paper.

Acknowledgements

This research was conducted with support from the Charles Pankow Foundation (CPF) and the American Institute of Steel Construction (AISC), through CPF research grant #05-17 awarded to co-PIs Michel Bruneau, from University at Buffalo and Amit H. Varma, from Purdue University. The researchers are also grateful to members of the FEMA P695 Peer-Review Panel (Gregory G. Deierlein, Professor, Stanford University; Ron Klemencic, Chairman & CEO, Magnusson Klemencic

Associates (MKA), and; Rafael Sabelli, Principal and Director of Seismic Design, Walter P.Moore), and members of the Project Advisory Team (Larry Kruth, Vice President, American Institute of Steel Construction (AISC); John D. Hopper, Senior Principal/Director of Earthquake Engineering, MKA; Jim Malley, Senior Principal, Degenkolb Engineers; Bonnie Manley, Regional Director of Construction Codes and Standards, American Iron and Steel Institute (AISI), and; Tom Sabol, Principal, Englekirk Institutional) for their technical guidance.

References

[1] AISC341. Seismic provisions for structural steel buildings. ANSI/AISC 341-16, American Institute of Steel Construction, Inc., Chicago, Illinois; 2016.
[2] Alzeni Y, Bruneau M. Cyclic inelastic behavior of concrete filled sandwich panel walls subjected to in-plane flexure. Technical Rep. MCEER 14-009, MCEER The State University of New York at Buffalo; 2014.
[3] Ang AH-S, Tang WH. Probability concepts in engineering: emphasis on applications in civil & environmental engineering. New York: Wiley; 2007.
[4] ASCE. Minimum design loads for buildings and other structures. Chicago, Illinois: American Society of Civil Engineers Inc.; 2016.
[5] Baker JW. Efficient analytical fragility function fitting using dynamic structural analysis. Earthquake Spectra 2015;31(1):579–99.
[6] Broberg M, Shafaei S, Kizilarslan E, Varma A, Bruneau M. Non-linear analysis models for filled composite coupling beams in coupled composite plate shear walls. TBD 2021. In preparation.
[7] Broberg M, Shafaei S, Kizilarslan E, Seo J, Varma AH, Bruneau M, Klemencic, R. Capacity design requirements for seismic design of coupled composite plate shear walls – concrete filled (CC-PSW/CF). J Struct Eng (2021), to be submitted for review; 2021.
[8] Bruneau M, Varma AH, Kizilarslan E, Broberg M, Shafaei S, Seo J. R-Factors for Coupled Composite Plate Shear Walls /Concrete Filled (CC-PSW/CF). Charles Pankow Foundation Grant # 05-17, McLean, Virginia, 419pp; 2019, Accessed from: https://www.pankowfoundation.org/05-17-r-factors-for-coupled-composite-plate-shear-wallsconcrete-filled-coupled-cpsw/cf.
[9] FEMA. FEMA P695: Quantification of building seismic performance factors. Applied Technology Council. Federal Emergency Management Agency; 2009.
[10] Ibarra LF, Medina RA, Krawinkler H. Hysteretic models that incorporate strength and stiffness deterioration. Earthquake Eng Struct Dyn 2005;34(12):1489–511.
[11] Kizilarslan E, Broberg M, Shafaei S, Varma AH, Bruneau M. Non-linear analysis models for Composite Plate Shear Walls-Concrete Filled (C-PSW/CF). J Constructional Steel Res 2021;106803. https://doi.org/10.1016/j.jcsr.2021.106803.
[12] Korlapati SCR, Raman R, Bruneau M. Modeling and test data uncertainty factors used in prior FEMA P695 studies. ASCE, Under Review 2020.
[13] PEER T. Guidelines for performance-based seismic design of tall buildings. PEER Report No. 2010/05, University of California Berkeley, USA; 2010.
[14] Shafaei S, Varma AH, Seo J, Klemencic R. Cyclic lateral loading behavior of composite plate shear walls / concrete filled (C-PSW/CF). J Structural Eng, ASCE 2021. https://doi.org/10.1061/(ASCE)ST.1943-541X.0003091.
[15] Zhang K, Varma AH, Malushte SR, Gallocher S. Effect of shear connectors on local buckling and composite action in steel concrete composite walls. Nucl Eng Des 2014;269:231–9.
[16] Shafaei S, Varma AH, Broberg M, Klemencic R. Modeling the cyclic behavior of composite plate shear walls/concrete filled (C-PSW/CF). J Constructional Steel Res 2021;184:106810. https://doi.org/10.1016/j.jcsr.2021.106810.